

Biophysics

A computer model of intracranial pressure dynamics during traumatic brain injury that explicitly models fluid flows and volumes*

W. Wakeland^{1,2} and B. Goldstein³

¹ Systems Science Ph.D. Program, Portland State University, Portland, OR, USA

² Biomedical Signal Processing Laboratory, Portland State University, Portland, OR, USA

³ Complex Systems Laboratory, Oregon Health and Science University, Portland, OR, USA

Summary

A model of intracranial pressure (ICP) dynamics that uses fluid volumes as primary state variables is presented, along with clinical data for two subjects with elevated ICP. The data includes annotations to indicate the precise timing of clinical changes in cerebral spinal fluid drainage, head of bed elevation, and minute ventilation. The response to changes in the clinical parameters was used to calibrate the model to correspond to specific subjects by estimating values for key characteristics such as hematoma volume and CSF uptake resistance. The error in mean ICP predicted by the model was less than 2 mmHg when cerebral spinal fluid is drained and the head of bed elevation was increased. The error in mean ICP predicted by the model exceeded 5 mmHg during an episode when the head of bed was decreased and also during a reduction in minute ventilation. The estimated values for hematoma volume and other subject characteristics were plausible but could not be verified empirically.

Keywords: Intracranial pressure; mathematical model; simulation; clinical data.

Introduction

There are several clinical treatment options for elevated ICP following severe traumatic brain injury (TBI). These include drainage of cerebral spinal fluid (CSF) via a ventriculostomy catheter, raising the head-of-bed (HOB) elevation to 30° to promote jugular venous drainage, and mild hyperventilation [1]. However, it is currently impossible to accurately and quantitatively predict how a subject will respond to a particular combination of therapeutic interventions. In addition, under certain conditions treatments may exhibit side effects that can worsen the subject's overall

condition. Tools are needed that help clinicians contend with these complex interactions. Unfortunately, the complexity of most of the simulation models reported in the literature limits their clinical usefulness.

Materials

Data was acquired from two subjects. Subject 1 was a 3-year-old female who was in a motor vehicle accident. She suffered a severe closed head injury and was found to be pneic when paramedics arrived at the scene. Her GCS at the scene was 4. She was transferred to a local community hospital where CT scan revealed a large right-sided epidural hematoma. In the emergency room she was noted to have a right pupil that was fixed, dilated and unresponsive to light, and her GCS was 3. She was tracheally intubated and taken to the operating room where the epidural hematoma was evacuated. She was then transported by helicopter to the pediatric intensive care unit (PICU) where a ventriculostomy catheter was placed. In the PICU she had equal, round, and mid-position pupils that were reactive to light. She had no spontaneous movements, no cough or gag reflex, and exhibited extensor posturing with painful stimulus. She required intravenous infusions of isotonic solutions, dopamine, dobutamine and epinephrine to maintain her blood pressure. She showed signs of severe anoxic/ischemic brain and multi-organ injury. On hospital day 2, her right pupil again became fixed, dilated and unresponsive to light. Repeat CT scan showed severe cerebral edema and cerebellar infarct. Due to the irreversible nature of her brain injury, supportive therapy was withdrawn by the family.

Subject 2 was an 8-year-old female who was a restrained passenger in a motor vehicle accident. On arrival to a local emergency hospital, she was moaning, and had a Glasgow Coma Scale (GCS) score of 8. She was tracheally intubated and transferred to the PICU. A cranial CT scan demonstrated diffuse axonal injury with no intra- or extracranial hemorrhage. The GCS in the PICU was 6. Pupils were 2 mm and reactive bilaterally. An intraventricular catheter was placed for ICP monitoring. Initial ICP ranged between 15–17 mmHg. The patient also had a left mandibular fracture and facial avulsion. The patient remained on a ventilator in the PICU and her ICP rose to a maximum of 38 mmHg by day 3. She was treated with mild hyperventilation (PaCO₂ 32–35 mmHg) and intravenous mannitol

* This research was supported in part by the Thrasher Research Fund.

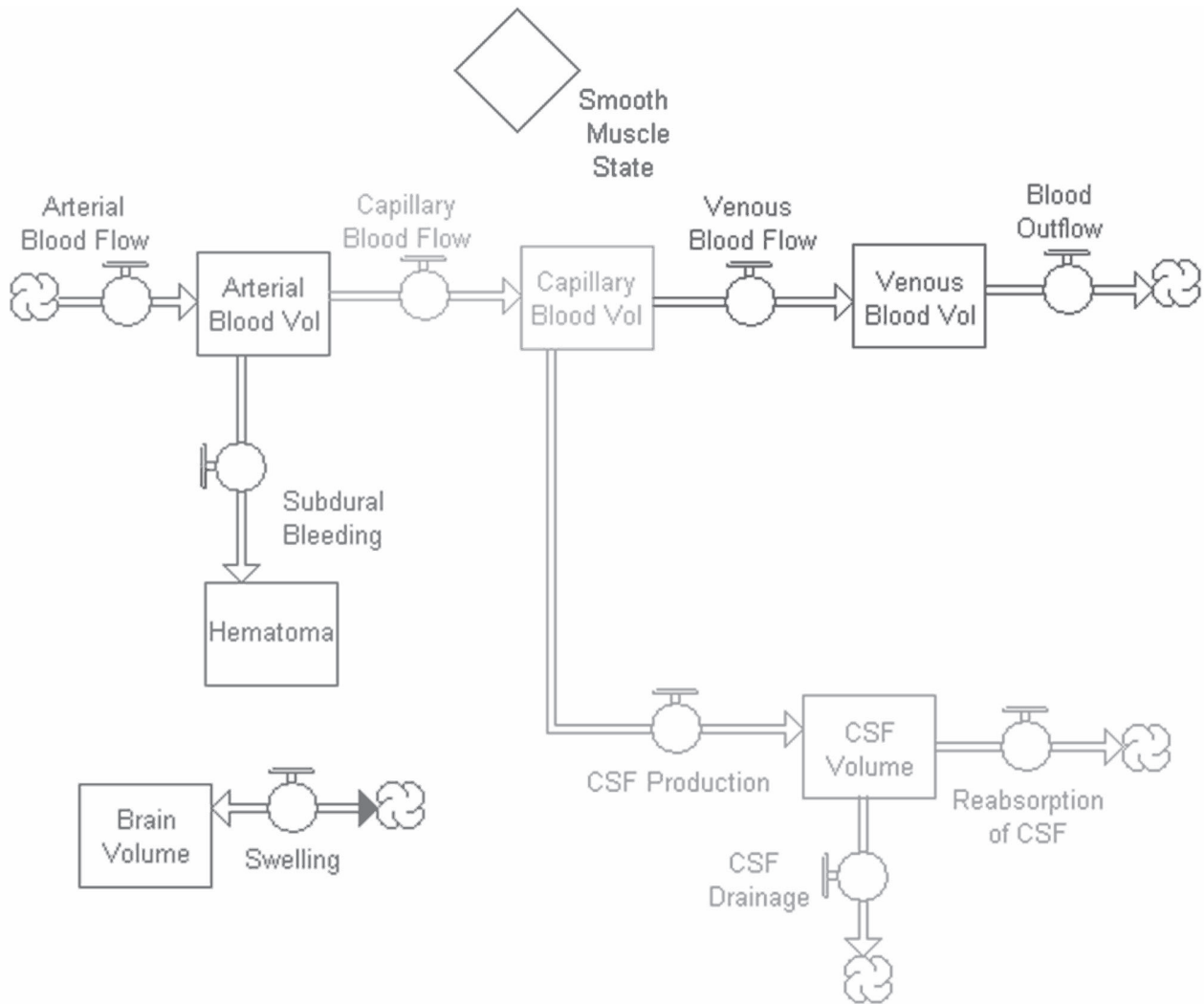


Fig. 1. Model state variables and flows. Fluid volumes are represented by rectangles, and fluid flows are represented by double arrows with a circular “valve-like” symbol superimposed on them to indicate that flows are variable. Brain swelling, the rate of change of brain volume, is also represented as a flow. The state of auto regulation is shown as a diamond, representing a submodel in this simulation software

(0.25 gram/kg IV every 3 hours). On day 5 she followed commands and was purposeful in all movements and was successfully extubated. She was transferred to the general pediatric ward on day 7, and then to a rehabilitation center on hospital day 9.

Methods

We developed a mathematical model that treats fluid volumes as the primary state variables. This is different from ICP dynamic models in the literature that treat pressures as the state variables [2, 5, 7]. To calibrate the model, we estimated a number of model parameters, including the volume and rate of change of an intracranial hematoma, CSF absorption resistance, and autoregulatory characteristics. Intra- and extracranial flows and pressures were calculated from the values of the state variables and the parameters, both fixed and estimated. Figure 1 shows the model state variables and flows, and how they are related.

Blood pressures are computed from the blood volumes and their respective compliances as shown in Equations 1–3.

$$P_{a\ ic} = P_{ic} + V_a/C_a \tag{1}$$

$$P_{c\ ic} = P_{ic} + V_c/C_c \tag{2}$$

$$P_{v\ ic} = P_{ic} + V_v/C_v \tag{3}$$

where:

- $P_{a\ ic}$ = pressure in the intracranial arteries
- P_{ic} = intracranial pressure (ICP)
- V_a = arterial blood volume
- C_a = arterial compliances
- $P_{c\ ic}$ = pressure in the intracranial capillaries
- V_c = capillary blood volume
- C_c = capillary compliances
- $P_{v\ ic}$ = pressure in the intracranial veins
- V_v = venous volume
- C_v = venous compliances

P_{ic} is computed as shown in Equation 4, based on the total intracranial volume and the pressure volume index (PVI) as defined by Marmarou [3]: the additional volume needed to cause a 10-fold increase in P_{ic} .

$$P_{ic} = P_{icb} * 10^{(V_{ic} - V_{icb})/PVI} \quad (4)$$

where: P_{icb} = baseline ICP for the subject
 V_{ic} = total cranial volume
 V_{icb} = base cranial volume

To model cerebrovascular autoregulation (CAR), the resistance at the arterioles changes rapidly, but within physiological limits, in order to adjust the cerebral blood flow to match metabolic needs, as indicated in Equations 5–7.

$$S_{sm} = \int^t \left[(F_{cap} - f_i) + \frac{1}{S_{sm}^3} + \frac{1}{(1 - S_{sm})^3} \right] * g \quad (5)$$

$$R_{cap} = \gamma * S_{sm} \quad (6)$$

$$F_{cap} = \frac{(P_{aic} - P_{cic})}{R_{cap}} \quad (7)$$

where: S_{sm} = smooth muscle state (\sim resistance, mmHg/ml/min;
0 = fully dilated, 1 = max. constriction)
 F_{cap} = capillary blood flow
 f_i = indicated blood flow
 g = cerebrovascular autoregulation gain (dimensionless)
 R_{cap} = capillary resistance
 γ = conversion factor (dimensionless)

The cubic terms in Equation 5 force the smooth muscle state to remain in the range [0, 1]. The CAR logic responds to changes in indicated blood flow needs due to diurnal variation, and changes in ICP, respiratory rate, arterial blood pressure, and HOB elevation.

The model also incorporates logic to reflect intracranial pathology such as intracranial hemorrhage and cerebral edema, and to reflect therapeutic interventions such as CSF drainage, elevation of the HOB, and changes in PaCO₂ using a proxy variable of minute ventilation (defined as the respiratory frequency \times tidal volume). For this preliminary report, we will only present data on changes in respiratory frequency when tidal volume was held constant. The flow rate for CSF drainage, F_{CSF} is modeled as shown in Equation 8.

$$F_{csf} = \frac{(P_{ic} - P_t)}{r_c} \quad (8)$$

where: F_{csf} = rate of cerebrospinal fluid drainage
 P_t = pressure at the terminus of the drainage system
(a function of its elevation)
 r_c = resistance of the catheter

The pressure differential, ΔP , due to changing HOB elevation is calculated as shown in Equation 9.

$$\Delta P = d * \sin(\theta) * \frac{\text{mmHg}}{\text{mmH}_2\text{O}} \quad (9)$$

where: ΔP = pressure difference
 d = distance between the heart and the head
 θ = head of bed angle

ΔP is subtracted from both the systemic arterial pressure and the systemic venous pressure to determine the external arterial and venous pressure at the cranial vault.

The impact of changing the PaCO₂ using a proxy variable of respiratory frequency (i.e., the ventilator rate) is much more complex (cf. [6]). We use the logic shown in Equations 10 and 11 to calculate the indicated blood flow that serves as input to the CAR logic.

$$f_i = k_1 + \alpha * (\text{PaCO}_2 - S) \quad (10)$$

$$\text{PaCO}_2 = \text{MOV}[(k_2 - \beta * VR), t_c] \quad (11)$$

where: k_1 = baseline blood flow
 α = flow multiplier
PaCO₂ = actual CO₂ pressure
 S = setpoint for CO₂ pressure
MOV(x, t) = moving average of variable x with averaging period t
 k_2 = offset for CO₂ pressure
 β = conversion factor from respiration rate to CO₂ pressure
VR = respiration rate in breaths per minute
 t_c = time constant

The model was calibrated to specific subjects based on recorded clinical data, including ICP, arterial blood pressure, and central venous pressure. The data used to calibrate the model was clinically annotated to indicate the exact timing of events such as changes in ventilator rate, CSF drainage and amounts, and changes in HOB elevation from 0° to 40° in 10° increments. Details of the data acquisition system were reported previously by Goldstein *et al.* [3]. Data for this report included both retrospective, non-annotated data as well as prospectively collected physiologic signals following an experimental protocol that included random changes to the height of the CSF drainage system, HOB elevation, and minute ventilation.

Results

Figure 2 shows the clinical data from the two subjects that was used to calibrate the model. Figure 2a shows the ICP signals recorded during three episodes of CSF drainage for Subject 1. These signals have been lowpass filtered to remove the pulsatile component, and synchronized in the time domain so that the point of drainage occurs at minute 5. Figure 2b shows the ICP signal recorded for Subject 2 when the HOB was changed from 30° to 0° and then back to 30°. Figure 2c shows the ICP signal recorded for Subject 2 when the ventilation rate was changed from 15 breaths per minute (bpm) to 12 bpm and then back to 15 bpm.

The model was calibrated to fit Subject 1 using the clinical data shown in Figure 2a. The estimated parameters were: *Initial intracranial hematoma volume* (24 mL), *hematoma volume increase rate* (0 mL/min.), *CSF drainage volume* (6.5 mL), and *CSF absorption resistance* (160 mmHg/mL/min). Figure 3a shows the ICP response to treatment in the model compared with the actual data. The error is less than 2 mmHg throughout the episode. On the other hand, the estimated *CSF absorption resistance* is much higher than typically reported and would normally be consistent with a higher steady state ICP value. In this case however, periodic CSF drainage therapy was employed to maintain ICP below its steady state value.

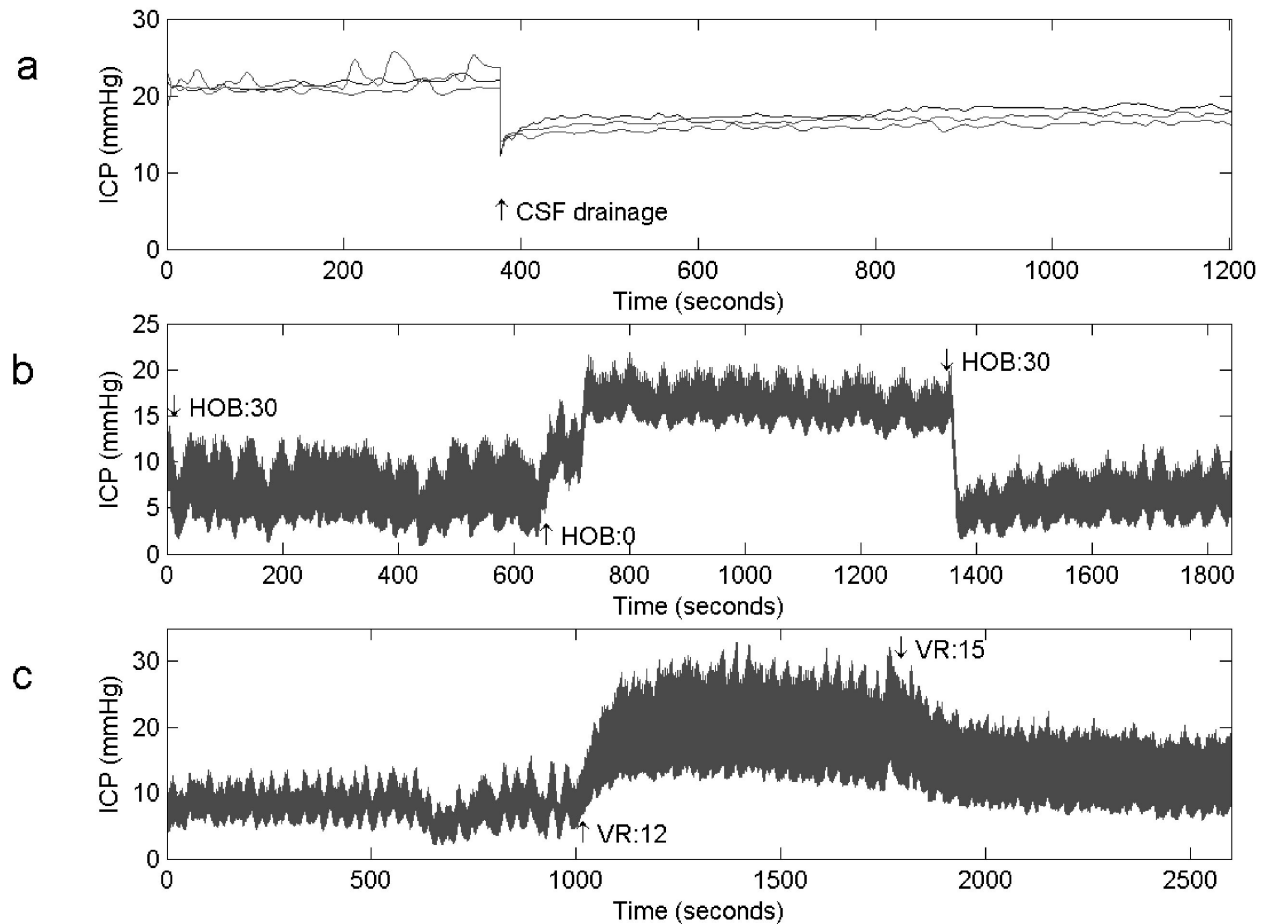


Fig. 2. Clinically recorded ICP signals. (a) ICP before and after CSF drainage for subject 1. (b) ICP during head of bed change for subject 2, from 30° to 0° and then from 0° to 30°. (c) ICP during respiration change for subject 2, from 15 breaths per minute (bpm) to 12 bpm and then from 12 bpm to 15 bpm

Next, the model was calibrated to fit Subject 2, using the data shown in Figure 2b. The estimated parameters included: *Initial intracranial hematoma volume* (6 mL), *hematoma increase rate* (.5 mL/min.), *CSF absorption resistance* (24 mmHg/mL/min), and estimated *distance from heart to brain* (45 cm). Figure 3b shows the ICP calculated by the model for this episode, compared to clinical data. During the first stage, the error is greater than 5 mmHg at some time points. During the second stage, the error is less than 2 mmHg.

The model was then further calibrated to Subject 2 based on the data collected during changes in respiratory frequency (Figure 2c). The previously-estimated parameters were retained, and the new data was used to estimate parameters associated with the CAR logic, including α (75 ml/mmHg), S (34 mmHg), k_2 (64 mmHg), β (2 mmHg-breaths/min.) and t_c (2.5

minutes). Figure 3c shows the ICP calculated by the model for this episode, compared to the clinical data. The error is greater than 5 mmHg.

Discussion

Our main finding was that this first generation ICP dynamic model was able to accurately replicate the subject's response to therapeutic intervention using CSF drainage and HOB elevation, but not following changes in respiratory frequency. The mean ICP calculated by the model for Subject 1 is very similar to the actual mean ICP recorded during their CSF drainage episodes. The large value for the estimated CSF absorption resistance implies a significant impediment to flow and/or absorption. This may be due to the initial injury, subsequent cerebral edema, or a combination. The model was also able to replicate Subject 2's overall

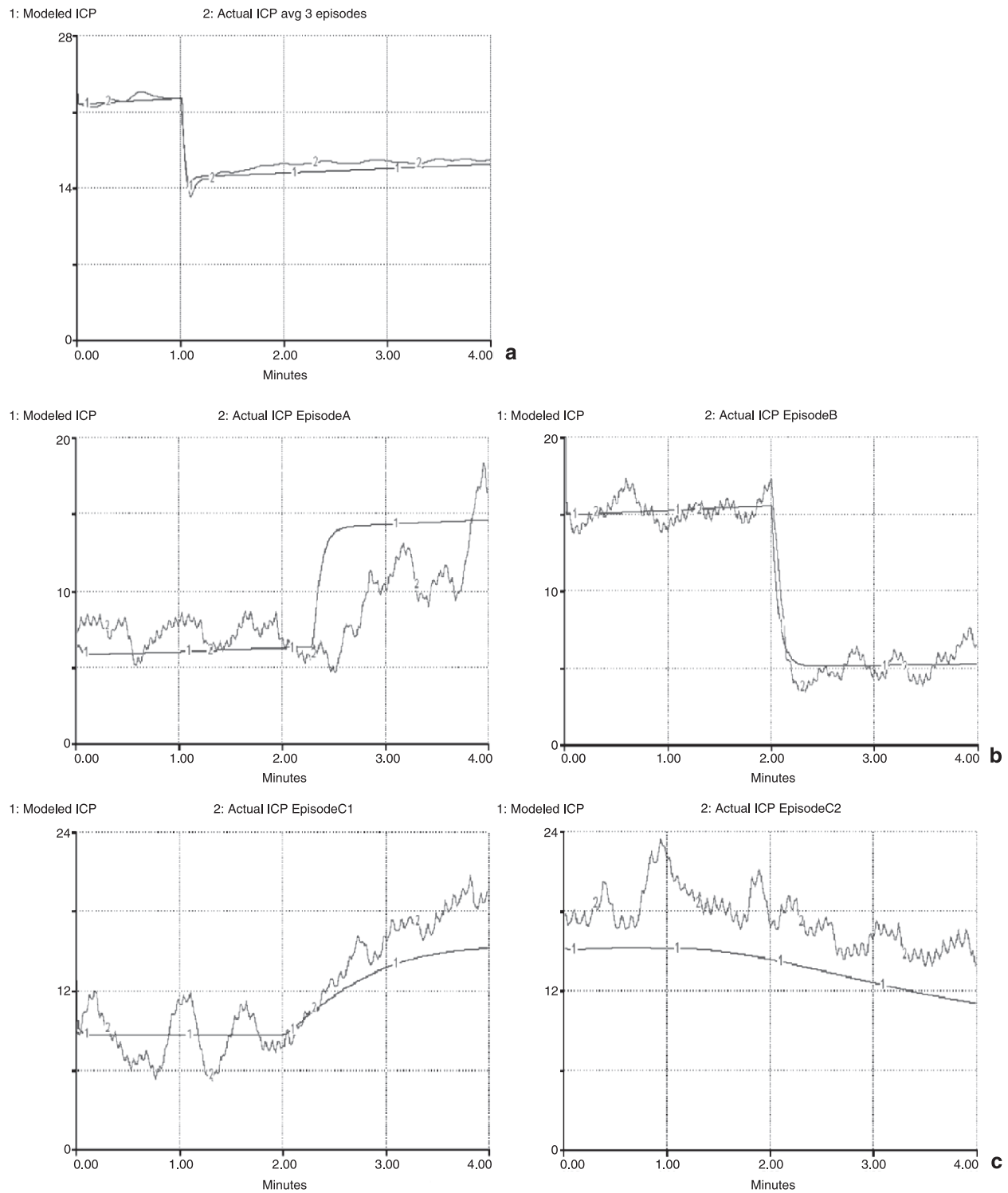


Fig. 3. Calculated vs. Recorded ICP (mmHg). (a) ICP before and after CSF drainage for subject 1. (b) ICP during head of bed change for subject 2, from 30° to 0° and then from 0° to 30°. (c) ICP during respiration rate change for subject 2, from 15 breaths per minute (bpm) to 12 bpm and then from 12 bpm to 15 bpm

ICP response to changes in HOB elevation, especially the response to raising the HOB. The modeled ICP response when HOB was lowered was less accurate. This is most likely due to the multiple autoregulatory mechanisms with differential responses triggered when the HOB is lowered and ICP begins to increase. These mechanisms currently are not incorporated in the model. The model was also not able to fully replicate the ICP signal for Subject 2 during changes in respiratory frequency. This may be due to the simplified CAR logic – indicating the need to enhance this portion of the model, or that respiratory frequency is a poor proxy for PaCO₂.

Other researchers have also recently focused their attention on multiple autoregulatory mechanisms. For example, Ursino and Magosso [8] demonstrate that three distinct CAR mechanisms are “. . . necessary to provide good reproduction of autoregulation to cerebral perfusion pressure changes.” These mechanisms include reactions to CO₂ changes, the reaction to tissue hypoxia, and a mechanism that responds to pressure changes in the large pial arteries and to flow rate in the small pial arteries. This latter mechanism might correspond to myogenic or neurogenic regulation, endothelium dependent factors, or other processes. Simulation results are validated against data reported in the literature. The reaction to tissue hypoxia was noted as being particularly complex, as we found in the present study. Another example is a recently-published mathematical model of ICP dynamics by Lakin, *et al.* [4] that incorporates, in addition to CAR mechanisms, the regulation of systemic vascular pressures by the sympathetic nervous system, and the regulation of CSF production in the choroid plexus. Simulation results are inspected for reasonableness but not com-

pared to clinical data. According to the authors, the additional autoregulatory mechanisms they describe are needed to accurately represent normal physiology as well as pathological conditions. The present study supports their assertion.

Acknowledgments

The authors greatly appreciate the support and assistance received from Mateo Aboy, Louis Macovsky, James McNames, and the Thrasher Research Foundation.

References

1. Adelson P *et al* (2003) Guidelines for the acute medical management of severe traumatic brain injury in infants, children and adolescents. *Ped Crit Care Med* 4(3)
2. Czosnyka M, Piechnik S, Richards H, Kirkpatrick P, Smielewski P, Pickard J (1997) Contribution of mathematical modeling to the interpretation of bedside tests of cerebrovascular autoregulation. *J Neurosurg* 63: 721–731
3. Goldstein B *et al* (2003) A physiologic data acquisition system and database for the study of disease dynamics in the intensive care unit. *Crit Care Med* 31: 433–441
4. Lakin W, Stevens S, Tranmer B, Penar P (2003) A whole-body mathematical model for intracranial pressure dynamics. *Math Biology* 46: 347–383
5. Marmarou A, Shulman K, Rosende R (1978) A nonlinear analysis of compliance and outflow resistance of the cerebrospinal fluid system. *J Neurosurg* 48: 332–344
6. Phillis (ed) (1993) *The regulation of cerebral blood flow*. CRC Press, Boca Raton
7. Ursino M, Lodi CA (1997) A Simple mathematical model of the interaction between intracranial pressure and cerebral hemodynamics. *J App Physiol* 82(4): 1256–1259
8. Ursino M, Magosso M (2001) Role of tissue hypoxia in cerebrovascular regulation: a mathematical modeling study. *Ann of Biomedical Engr* 29: 563–574

Correspondence: Wayne Wakeland, Systems Science Ph.D. Program, PO Box 751, Portland, OR 97208, USA. e-mail: wakeland@pdx.edu